

## 6.5 Site-Specific Generalized Beamforming (SSGBF) applied to the Lop Nor test site

### *Introduction*

In the preceding NORSAR Semiannual Technical Summary we reported on our initial efforts to develop an optimized site-specific threshold monitoring (SSTM) system for the Lop Nor test site in China (Lindholt et al., 2002). Our aim was to calibrate all available high-quality seismic stations within regional distance, and supplement with the best IMS arrays at teleseismic distances. As a calibration data base, we used several past nuclear explosions at the test site, combined with nearby, well-recorded earthquakes.

We have now developed a site-specific Generalized Beamforming (SSGBF) approach to supplement the SSTM system for monitoring the Lop Nor test site. This paper describes the methodology and initial results using the SSGBF approach. We also comment briefly on the relative merits of the two approaches (SSTM and SSGBF), and the extent to which they complement each other in this particular case study.

### *Development of site-specific GBF*

The Generalized Beamforming (GBF) technique, originally developed by Ringdal and Kværna (1989), is now widely accepted as the most efficient method for associating seismic phases from a global or regional network. In a typical implementation, a large number of generalized “beams” are steered to the points in a global or regional grid. An automatic detector is applied to each station or array in the network, and a set of “box-car” functions is generated for each station, so that the non-zero parts of these functions correspond to a time interval around a detection. By adding these functions with appropriate weights and with time delays corresponding to the particular phase-station-grid point combination, one obtains a “beam” that may then be subjected to a detector algorithm.

A common feature of such implementations is the need to group the large number of individual beam “detections” so as to eliminate side-lobes and associate the detection group with an event at the correct hypocenter. This grouping, which can become quite complex, is clearly unavoidable when a large geographical region is to be monitored. However, if one is monitoring a particular site, such as a suspected nuclear test site, it is possible to simplify this procedure considerably, and at the same time optimize the parameter settings to ensure the best possible detection probability for the target site. This idea was first tested by Ringdal and Kværna (1993) to monitor the aftershocks of a large earthquake sequence occurring in Western Caucasus during the GSETT-2 experiment. They concluded that the approach showed a superior performance compared to the association procedures being employed at the four experimental international data centers operating during GSETT-2. In the present paper we elaborate further on this site-specific GBF (SSGBF) approach to monitor the Lop Nor test site.

### *Data base and analysis procedure*

The data base for this study has consisted of recordings by an experimental seismic network composed of stations and arrays at teleseismic as well as regional distances from the Lop Nor test site. We develop and test a parameter set calibrated towards the test site, and discuss the

SSGBF results in conjunction with the results from the site-specific threshold monitoring (SSTM) technique applied to the same site.

For the purposes of this study, 18 seismic stations (including 9 arrays) were initially chosen as shown in Fig. 6.5.1. These stations are a subset of the 23 stations used in the study by Lindholm et. al. (2002). Table 6.5.1 summarizes the station information and also lists the range of the azimuth and slowness parameters used for forming the beam towards the test site. Only P-phases are used in this study. We note that the slowness restriction is only defined for the array stations, whereas for the 3-component stations we do not impose any restriction on the slowness value. The azimuth restrictions are defined for all stations, and have been set to +/- 30 degrees of true azimuth.

The limits on arrival time tolerances are not defined in Table 6.5.1, since these tolerances are to a large extent dependent on the desired sharpness of the generalized beam. We have used the formula:

$$dT=S*R/111.13$$

where  $dT$  is the time tolerance in seconds,  $R$  is the desired beam radius in km and  $S$  is the P-phase slowness (in s/km) corresponding to the distance from the target site to the station being processed. If a beam radius of e.g. 50 km is desired, and the expected P-wave phase velocity at a given station is 8 km/s, then the assumed range of the time tolerance is approximately +/- 6 seconds.

In general, there is a trade-off between the sharpness of the generalized beam and the size of the tolerance intervals of the parameters. We have chosen to use fairly large tolerances, to ensure that there is only a small probability of missing real detections corresponding to an event at the site. In future studies, these parameters may be fine tuned to take advantage of those arrays and 3-component stations that are particularly well calibrated. For example, for well-calibrated stations the azimuth tolerances may be greatly narrowed, resulting in a reduced false association rate at no loss in detectability for real on-site events.

The beamforming procedure follows the GBF standard, except that only one generalized beam is formed in the site-specific case. The main steps are:

- Applying an automatic detector at each of the stations/arrays in the network
- Adding together weighted "box-car functions" representing the detector outputs with the appropriate restrictions on travel time, azimuth and slowness
- Applying a thresholding procedure on the resulting generalized beam

We have used 0-1 weights for the beamforming in our initial analysis, with standard (rectangular) box-car functions. In addition, we have made some experiment with using alternative functions (e.g. triangular functions centered at the expected arrival time). We will return to the results of these experiments in a later paper. For now, we proceed to present preliminary results using the standard approach.

**Table 6.5.1. The stations used for Site-Specific Generalized Beamforming processing of the Lop Nor test site. In order for a signal detection to be used as a candidates an event at the Lop Nor test site, its azimuth and slowness estimates has to be within the ranges given in the table. Notice that for three-component stations only the azimuth range is used.**

Station	Type	Delta	P travel time	Azimuth Range (deg)	Slowness Range (sec/deg)
ARCES	Array	42.47	478.2	60 - 124	5.5 - 12.5
ASAR	Array	77.16	719.2	300 - 359	3.0 - 9.0
CMAR	Array	24.64	326.8	305 - 359	6.3 - 12.3
FINES	Array	41.75	472.4	58 - 118	5.2 - 11.2
GERES	Array	51.41	548.6	42 - 102	6.3 - 12.3
HFS	Array	47.93	521.0	45 - 105	3.2 - 9.2
ILAR	Array	65.57	645.9	283 - 343	2.1 - 8.1
NORES	Array	48.84	528.5	50 - 110	4.9 - 10.9
MKAR	3C/Array	6.88	103.3	120 - 170	10.1 - 16.1
ARU	3C	24.43	322.8	84 - 144	NA
BRVK	3C	16.87	239.6	95 - 155	NA
KURK	3C	11.47	165.7	109 - 169	NA
KZA	3C	9.92	149.8	58 - 118	NA
NIL	3C	14.38	209.0	22 - 82	NA
TKM2	3C	9.68	146.0	63 - 123	NA
ULHL	3C	9.18	139.8	60 - 120	NA
ULN	3C	14.64	216.4	221 - 281	NA
USP	3C	10.51	156.6	65 - 125	NA

### *Preliminary results*

We present below some preliminary results in applying site-specific generalized beamforming to the Lop Nor test site in China. Two data sets for performance testing were compiled. The first data set covered one day (10 September 2001), and in these data the recordings of 4 explosions were scaled and embedded at some (but not all of) the stations (see Lindholm et. al., 2002). Secondly, a 10 day test period with data from August 2 through 11, 2001 was selected and data were collected for the stations.

#### *Example 1: 10 August 2001*

Our first example is the day 10 August 2001. Figs. 6.5.2 and 6.5.3 show the SSGBF traces for arrays and single stations respectively for that day. In Fig. 6.5.2, the peaks of the panels for each array represent detections that fall within the Lop Nor azimuth and slowness ranges given in Table 6.5.1. To align the detections we have subtracted the P travel-time from Lop Nor to the respective arrays. The network trace on top is calculated by adding boxcar functions surrounding each detection, using both the arrays of this figure and the three-component stations of Figure 6.5.3. In Fig. 6.5.3, the same type of display is shown, but only for the 3-component

stations. Furthermore, in Fig. 6.5.3, the top trace uses only detector information from the 3-component stations in the network.

Alerts (red diamonds) are declared when the network trace (the full network) has at least three matching detections, where at least one detections has to be at an array. The red diamonds at the individual arrays or 3-component stations on the two figures show detections that fall within the alert interval defined on the network trace. The event at 03:15 is located in northern Xinjiang, about 200 km north of the Lop Nor test site. It is interesting to note that this event triggers a clear detection on the generalized beam steered towards Lop Nor, even if the distance to the test site exceeds the beam coverage radius of 50 km. In practice, it is difficult to avoid such side lobe detections at nearby sites, and in any case, it may be useful to have indications on the beam trace that such nearby events may have occurred. The two alerts between 19:00 and 21:00 are caused by signals of unknown origin. Most likely these alerts are false alarms caused by coinciding detections at the different stations.

#### *Example 2: 5 August 2001*

As another example, Fig. 6.5.4 shows (in the top panels) SSGBF processing results for 5 August 2001. Only the arrays and the full network trace are shown. Two alerts are declared, and we note that several detections fall within the alert interval. However, these detections do not add constructively to the network trace, indicating that they were associated with an event *outside* the source region. At the bottom panel of Fig. 6.5.4 we show the corresponding SSTM results (presented by Lindholm et. al., 2002), having threshold peaks at the same times as the SSGBF network trace. These peaks are verified to be caused by events far from the Lop Nor test site, (Andaman Islands and Afghanistan, respectively).

#### *Example 3: 2 August 2001*

Our third example is similar to Example 2, but covers a “quiet” day (2 August 2001) during which there were no large seismic events globally, and no significant event near Lop Nor. The top panels of Fig. 6.5.5 show the SSGBF processing results. No alerts are declared. The corresponding SSTM, shown below the red line, has no significant peaks and a background level varying between 2.6 and 3.0.

#### *Example 4: 10 September 2001*

Our final example (Figs. 6.5.6 and 6.5.7) is the one day (10 September 2001) which contained the scaled, embedded events, and the combined network SSGBF trace (using all stations) is shown on top of each figure. In Fig. 6.5.6, which gives the standard display of the arrays and the combined network SSGBF traces, we note the large number of alerts declared automatically. A total of 11 alerts are declared for that day by the SSGBF method. These alerts correspond to the eight embedded explosions (scaled magnitudes 3.0 to 3.5), one additional trigger that turned out to be a real event near Lop Nor, and two alerts of unknown origin.

Fig. 6.5.7 shows a combination of SSGBF and SSTM results for the same day (10 September 2001) with scaled, embedded events. The top panel shows the SSGBF network trace for 10 September 2001. Below is shown the SSTM network trace for the same day. Red circles indicate events for which the SSTM processing issued an alert, whereas blue circles indicate events

for which an alert was not issued. Notice the good correspondence between the SSGBF alerts (red diamonds) and the SSTM alerts.

### *Conclusions*

From these tests the following preliminary observations can be stated:

- Out of the eight embedded explosions on 10 September 2001, six were flagged by the automatic SSTM detector, whereas all eight were flagged by the automatic SSGBF detector.
- The quiet day (2 August 2001) did not have any events flagged, neither by the SSTM nor the SSGBF detector.
- On 5 August 2001 the SSGBF as well as the SSTM method triggered on two large teleseismic events.

The above observations should be evaluated under the perspective that the study is of a very preliminary nature, and that further optimization and tuning of the SSGBF method is clearly possible. Furthermore, the addition of newly developed and planned IMS stations would contribute to a significant improvement in detector performance.

The false association problem of the SSGBF approach has not yet been evaluated in detail, but preliminary indications are that the likelihood of spurious associations is low, even with the fairly relaxed set of parameter tolerances used in this study. A more extensive study of this topic is being planned.

The combination of the SSTM and the SSGBF techniques appears to be a very promising new development. Each of these two approaches has its specific strengths. The SSTM technique has as its main strength the ability to display the real seismic field, without regard to “station detector performance”. On the other hand, the SSGBF technique takes advantage of the individual station detector outputs, and uses this combined information to narrow down the number of possible candidates for events in the target area.

From the above we conclude that the Site-Specific Generalized Beamforming performance tests for the Lop Nor test site were successful. It is expected that these initial tests will be followed by more detailed studies, where in particular the calibration parameters will be more firmly established and the combined benefits of the SSTM and the SSGBF methods will be further explored.

**Tormod Kværna**

**Erik Hicks**

**Frode Ringdal**

**References:**

- Lindholm, C., T. Kværna and J. Schweitzer (2002): Site-Specific Threshold Monitoring (SSTM) applied to the Lop Nor test site, *Semiannual Technical Summary, 1 July - 31 December 2001*, NORSAR Sci. Rep. 1-2002, Norway.
- Ringdal, F. and T. Kværna (1989): A multichannel processing approach to real time network detection, phase association and threshold monitoring, *Bull. Seism. Soc. Am.*, 79, 1927-1940.
- Ringdal, F. and T. Kværna (1993): Generalized Beamforming as a tool in IDC processing of large earthquake sequences, *Semiannual Technical Summary, 1 April - 30 September 1993*, NORSAR Sci. Rep. 1-93/94, Norway.

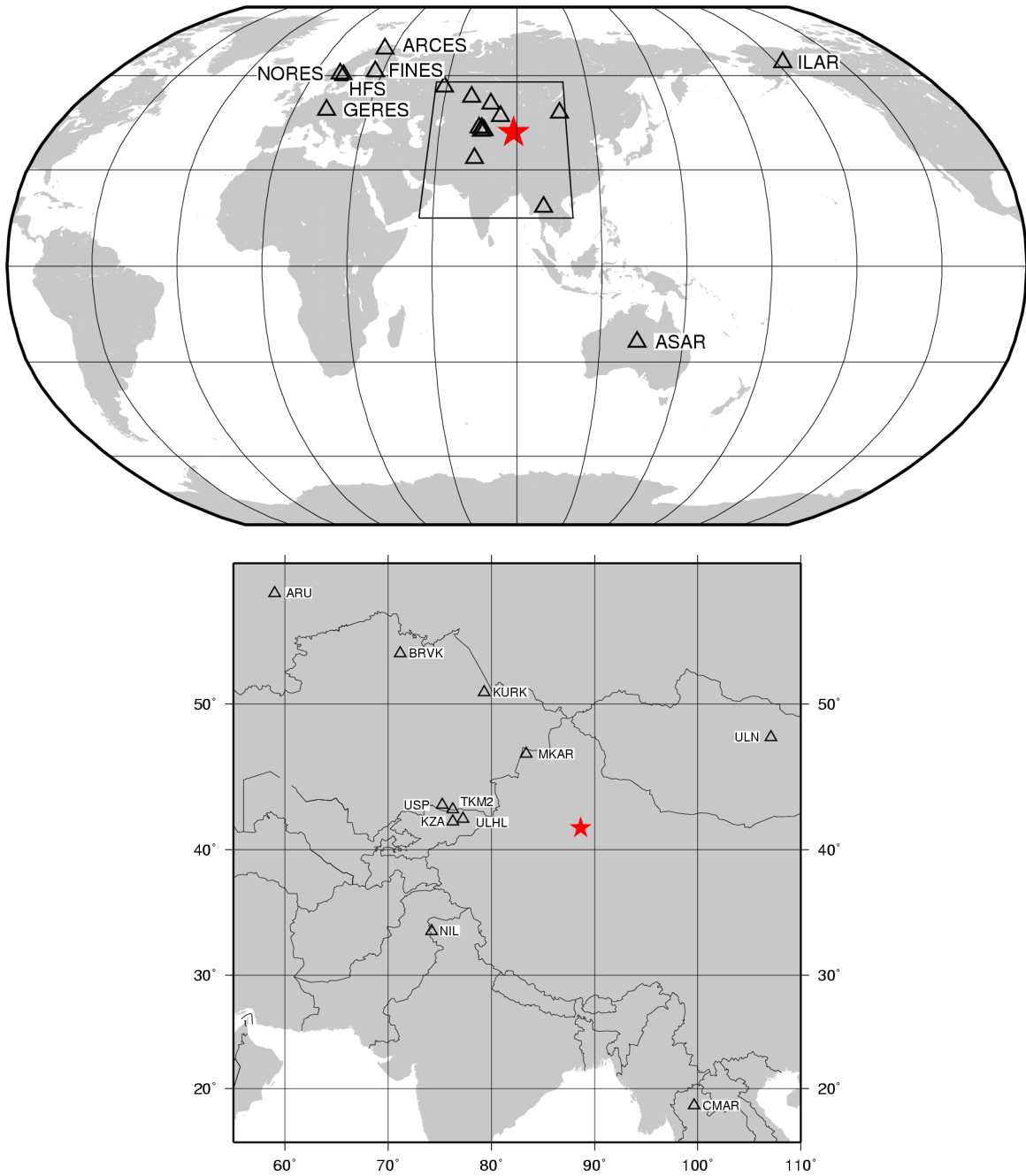


*Fig. 6.5.1. Maps showing arrays and stations used for Site-Specific GBF processing of the Lop Nor Test Site (indicated with red star).*

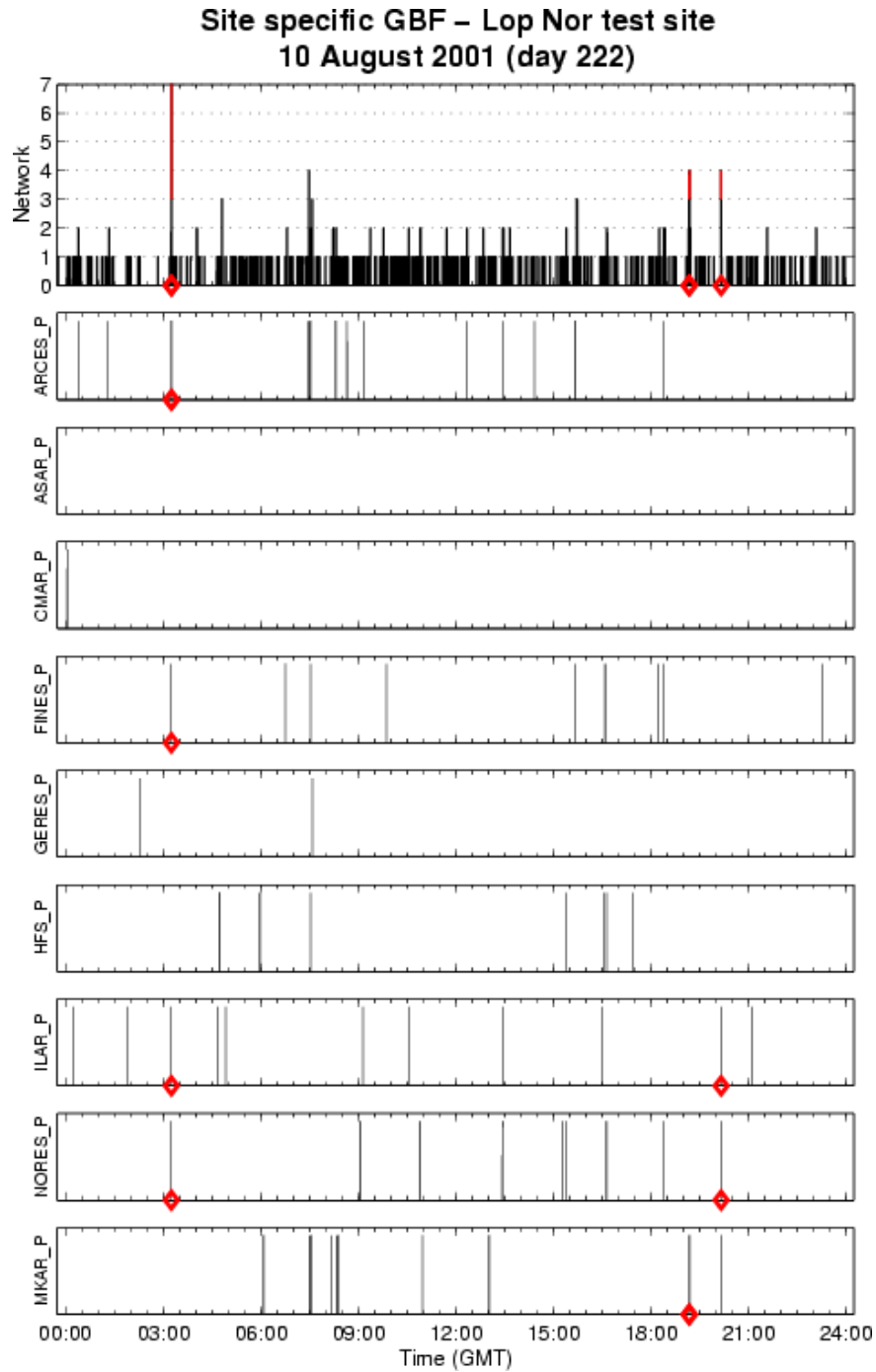


**Fig. 6.5.2.** The peaks of the panels for each array represent detections that fall within the Lop Nor azimuth and slowness ranges given in Table 6.5.1. To align the detections we have subtracted the P travel-time from Lop Nor to the respective arrays. The network trace on top is calculated by adding boxcar functions surrounding each detection, using both the arrays of this figure and the three-component stations of Figure 6.5.3. Alerts (red diamonds) are declared when the network trace has at least three matching detections, where at least one detections has to be at an array. The red diamonds at the individual arrays show detections that fall within the alert interval defined on the network trace. The event at 03:15 is located in northern Xinjiang, about 200 km north of the Lop Nor test site. The two alerts between 19:00 and 21:00 are caused by signals of unknown origin.



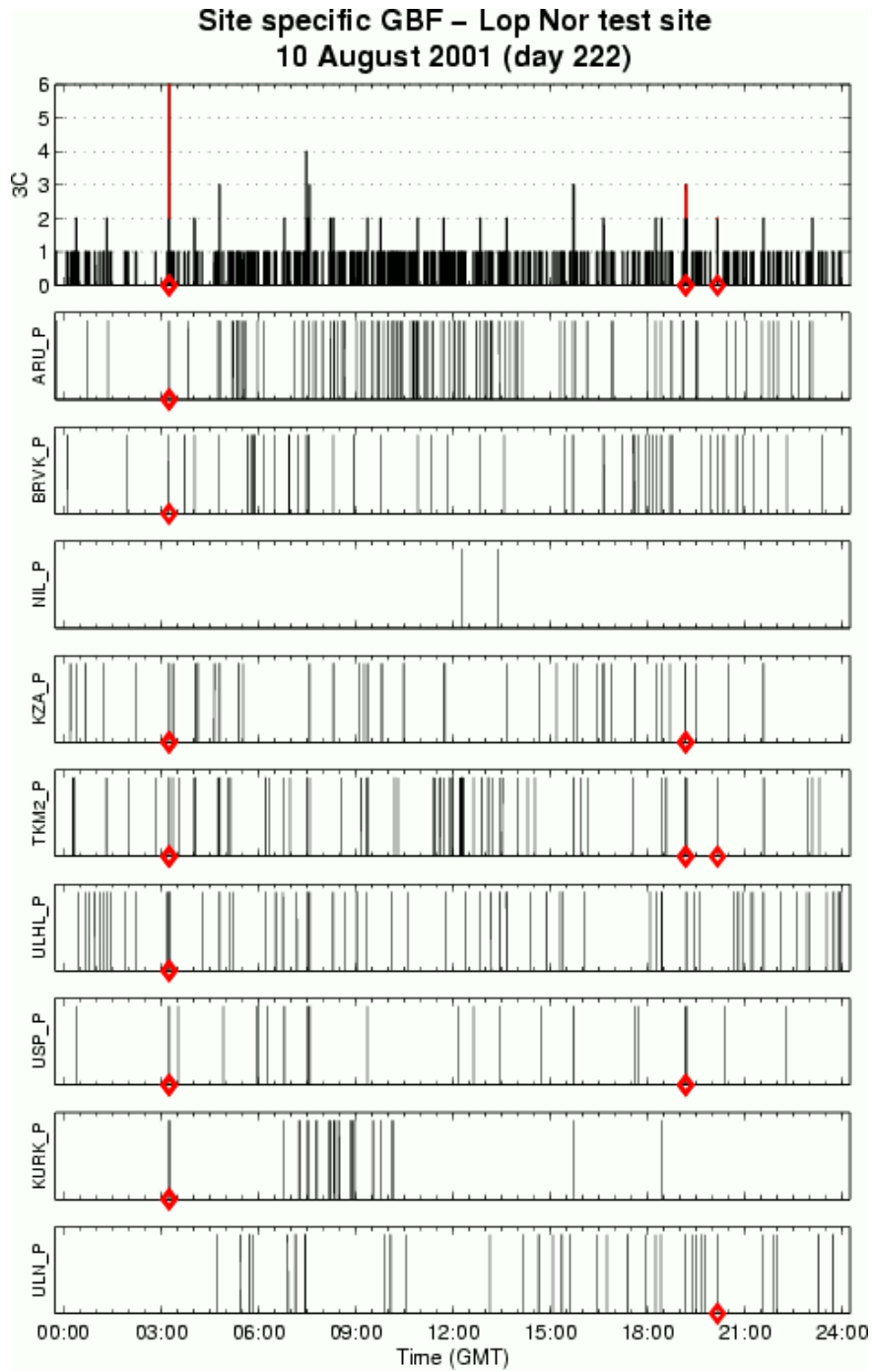


*Fig. 6.5.3. The peaks of the panels for each 3C station represent detections that fall within the Lop Nor azimuth ranges given in Table 6.5.1. To align the detections we have subtracted the P travel-time from Lop Nor to the respective stations. The 3C network trace on top is calculated by adding boxcar functions surrounding each detection, using the three-component stations only. The red diamonds at the 3C network trace and the individual stations show peaks that fall within the alert interval defined on the full network trace shown in Figure 6.5.2.*

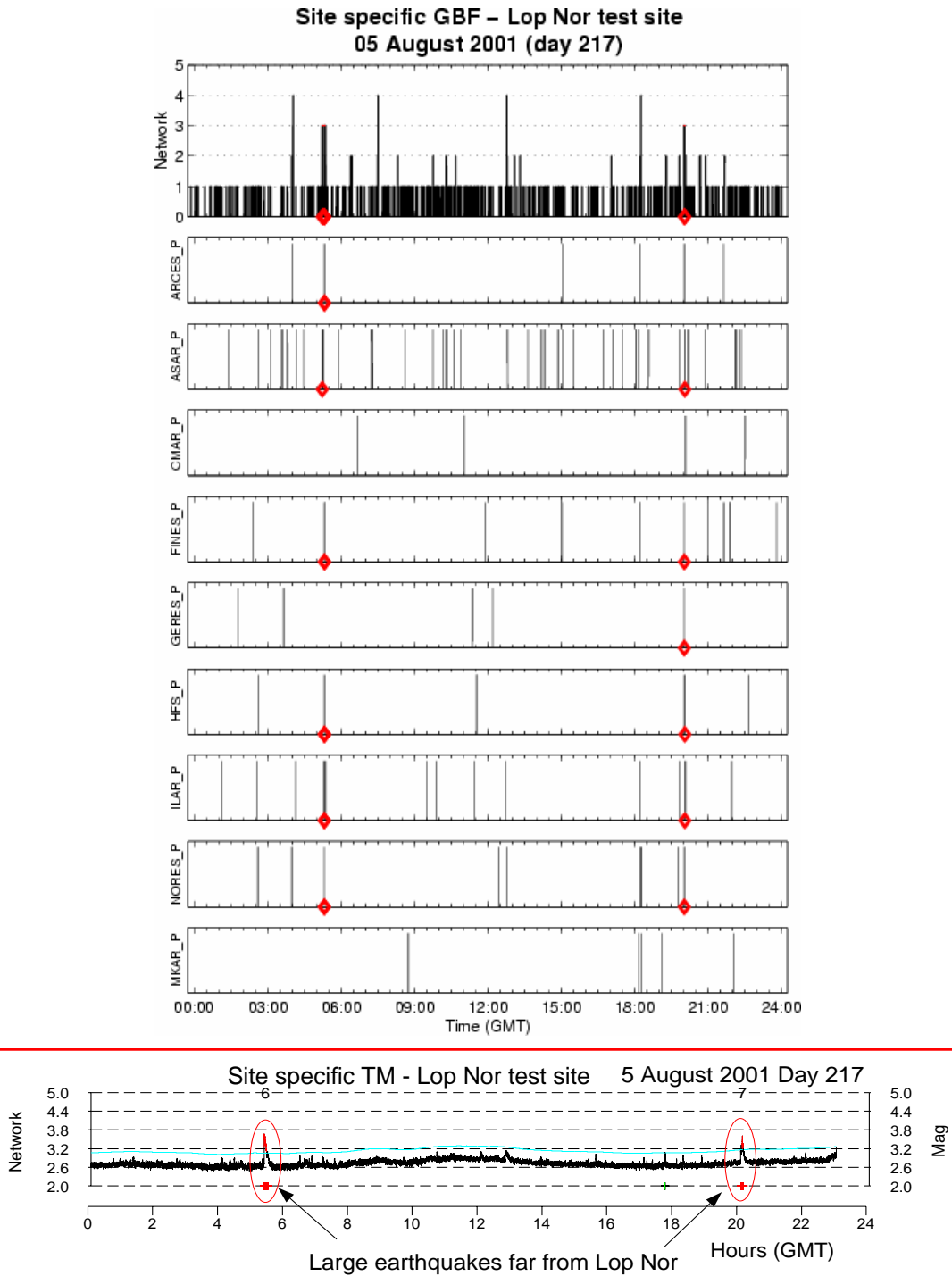


*Fig. 6.5.4. The top panels show SSGBF processing results for 5 August 2001. Two alerts are declared, and we find that several detections fall within the alert interval. However, these detections do not add constructively to the network trace, indicating an event outside the source region. Below the red line we show the corresponding SSTM results (presented in the previous NORSAR Semiannual Report), having threshold peaks at the same time as the SSGBF network trace. These peaks are verified to be caused by events far from the Lop Nor test site, respectively, Andaman Islands and Afghanistan.*

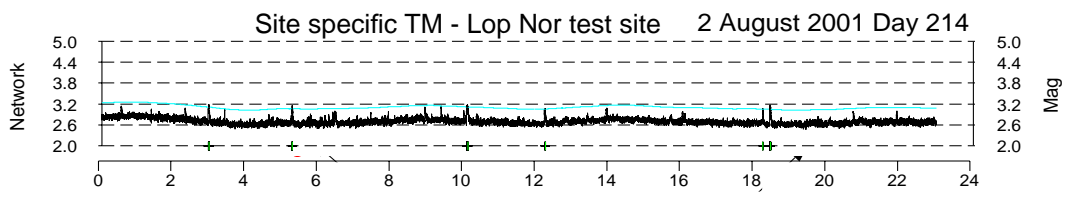
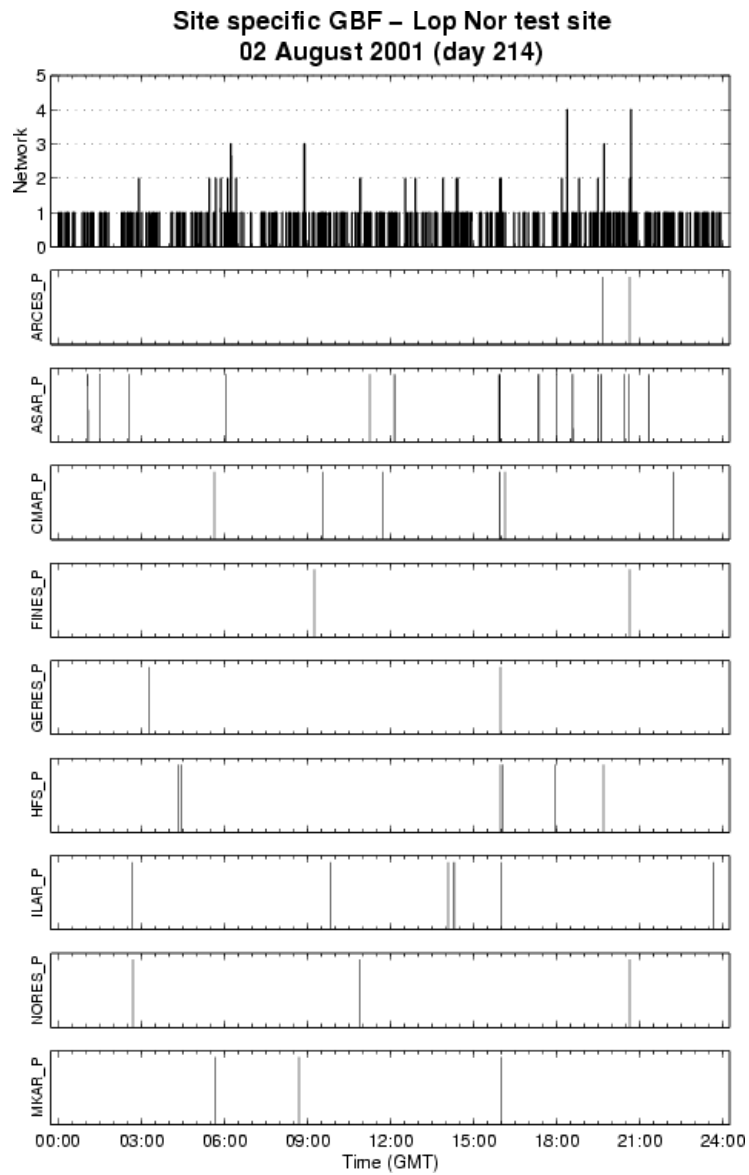


*Fig. 6.5.5. The top panels show SSGBF processing results for 2 August 2001. No alerts are declared. The corresponding SSTM, shown below the red line, has no significant peaks and a background level varying between 2.6 and 3.0.*

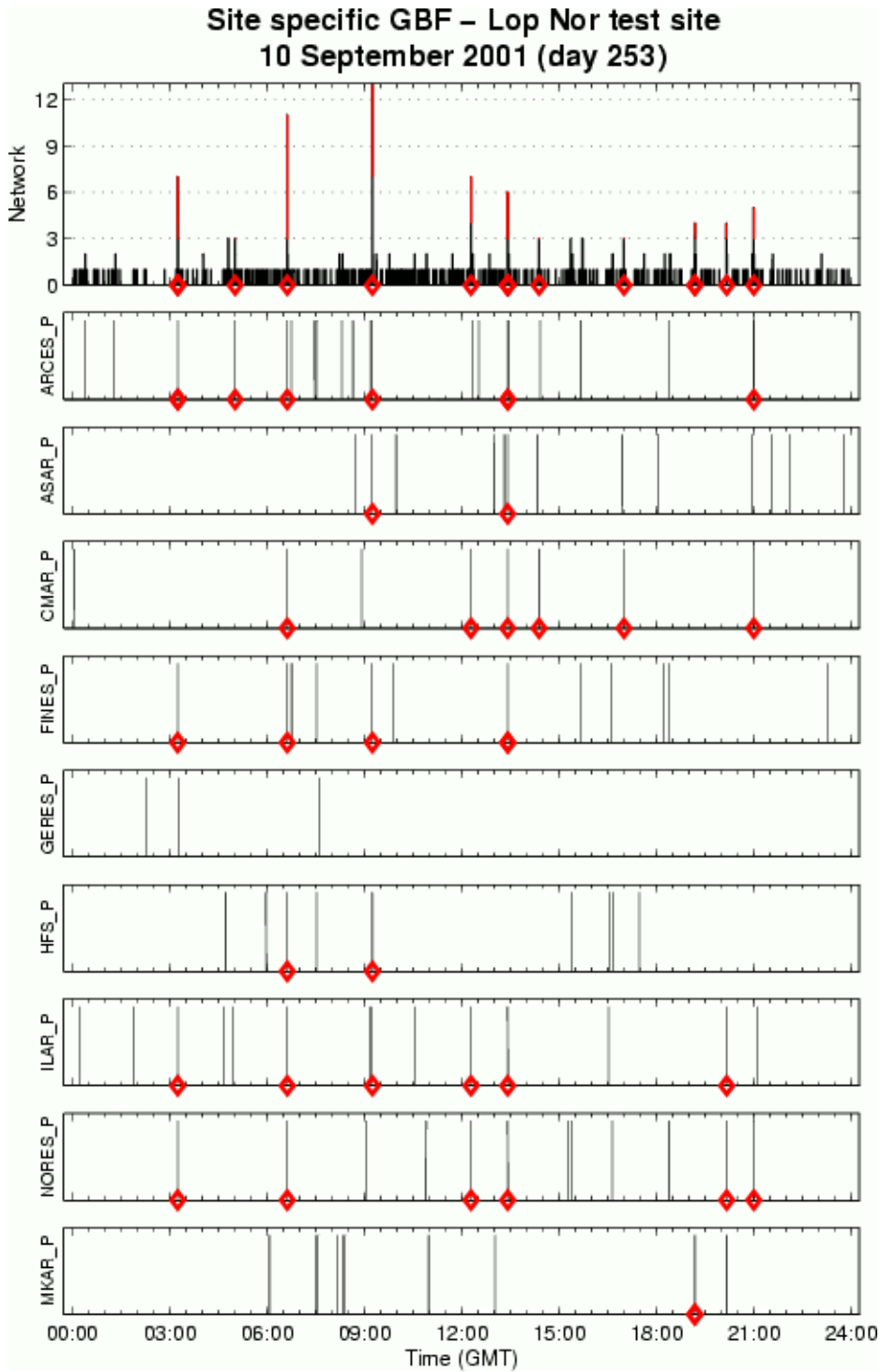


*Fig. 6.5.6. The top panels show SSGBF processing results for 10 September 2001, with several embedded Lop Nor event recordings scaled to magnitudes 3.0 and 3.5. Notice the large number of alerts declared.*

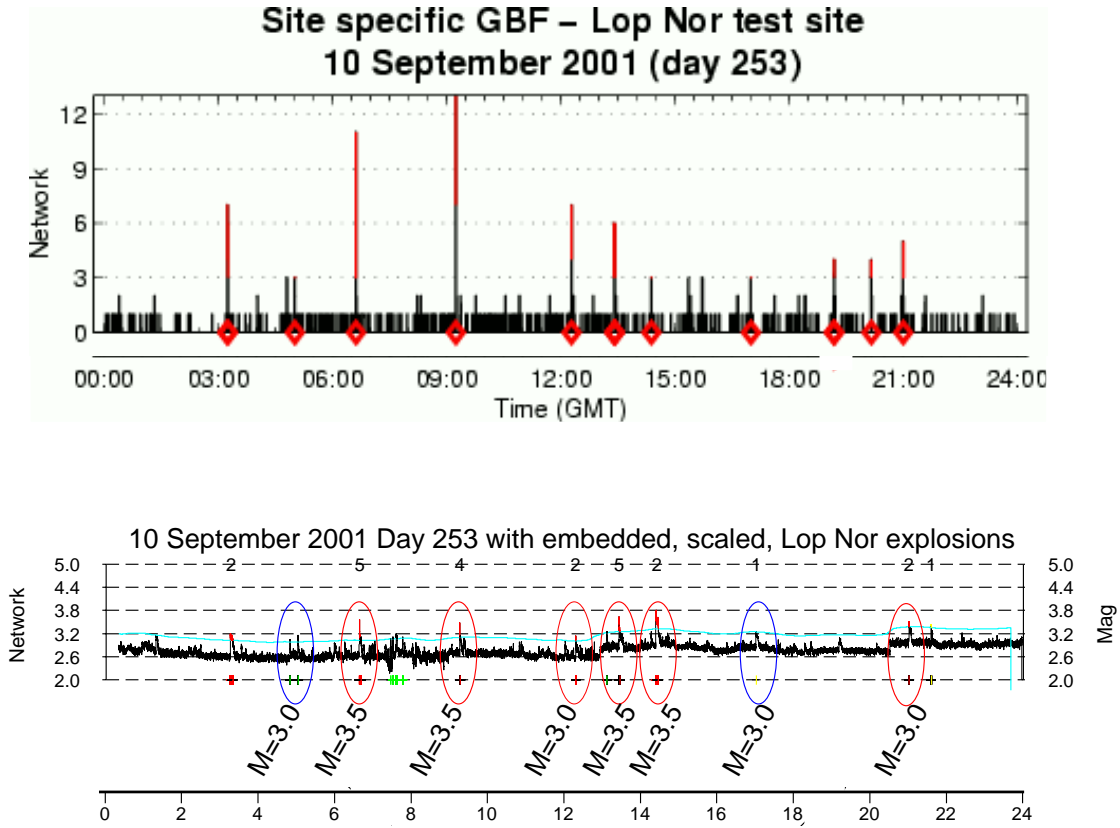


**Fig. 6.5.7.** The top panels show SSGBF network trace for 10 September 2001. Below is shown the Network SSTM trace for the same day. Red circles indicate events for which the SSTM processing issued an alert, whereas blue circles indicate events for which an alert was not issued. Notice the good correspondence between the SSGBF alerts (red diamonds) and the SSTM alerts. The event at 03:15 is located in northern Xinjiang, about 200 km north of the Lop Nor test site.